Electronic Supplementary Information

Use of flow field-flow fractionation and single particle inductively coupled plasma mass spectrometry for size determination of selenium nanoparticles in mixture

Luluil Maknun[a], Jitapa Sumranjit[b], and Atitaya Siripinyanond[a]*

[a]Department of Chemistry and Center of Excellence for Innovation in Chemistry, Faculty of Science, Mahidol University, Rama VI Road, Bangkok 10400, Thailand

Fax : +662-354-7151; Tel: +662-201-5195; E-mail: atitaya.sir@mahidol.ac.th

[b]National Nanotechnology Center (NANOTEC), 111 Phahonyothin Rd., Klongluang, Pathumthani 12120, Thailand

Table S1. Symmetrical flow field-flow fractionation operating conditions

FlFFF : PN-1021-FO	
FFF channel dimension (cm)	27.7 cm long x 2.0 cm wide x 250 µm thick
Carrier liquid	0.02 % (v/v) FL-70 and 0.02 % (w/v) NaN_3,
Channel flow rate (mL min^{-1})	1.2
Cross flow rate (mL min^{-1})	0.8
Equilibration time (min)	2.4
Membrane	10 kDa RC
Spacer (µm)	250
Injection volume (µL)	20

Table S2. Asymmetrical flow field-flow fractionation operating conditions

FlFFF : AF2000 Postnova Analytics			
FlFFF channel dimension	33.5 cm x 4.0 cm x 250 µm		
Carrier liquid	0.02 % (v/v) FL-70 and 0.02 % (w/v) NaN_3		
Membrane	10 kDa RC		
Spacer (µm)	350		
Injection volume (µL)	20		
Injection/Focusing			
Detector flow rate (mL min^{-1})	0.50	Cross flow rate (mL min^{-1})	0.80
Injection flow rate (mL min^{-1})	0.20	Injection time (min)	3.00
Focus flow rate (mL min^{-1})	0.10	Transition time (min)	0.50
1st Elution step			
Elution time (min)	2.00	Initial cross flow (mL min^{-1})	0.80
Elution type	constant		
2nd Elution step			
Elution time (min)	25.00	Initial cross flow (mL min^{-1})	0.80
Elution type	power	Exponent	0.20
3rd Elution step			
Elution time (min)	10.00	Initial cross flow (mL min^{-1})	0.00
Elution type	constant		

Table S3. ICP-MS operating conditions

PerkinElmer NexION 2000 ICP-MS	
Nebulizer	Concentric (MEINHARD® plus Glass, Type C)
Spray chamber	Glass Cyclonic at 2 ^{o}C
Injector	2.5 mm id
Nebulizer gas flow (L min^{-1})	0.85 - 1.0
Rf power (W)	1600
Dwell time (µs)	50
Scan Time	30
Analysis time (s)	60
Sample flow rate (mL min^{-1})	0.37
Monitored isotope (m/z)	^{80}Se
Transport efficiency	determined by using 60 nm of AuNPs

Factors affecting Sy-FlFFF performance

1. Effect of membrane materials on the particle membrane interaction

To evaluate the effect of membrane material on fractionation performance, we examined the use of two different types of membrane material which were regenerated cellulose (RC) membrane and polyethersulfone (PES) membrane that were predominantly used in FlFFF with using 0.02% FL-70 and 0.02% NaN_3 as carrier liquid. All are negatively charge membranes. We tested these membranes with two molecular weight cut off (MWCO), which were 1 kDa RC, 10 kDa RC, 1 kDa PES and 10 kDa PES. In order to examine particle-membrane interaction, two types of SeNPs were tested, including SeNPs coated by β-lactoglobulin (23.3 mV) as a representative of postively charged particle and SeNPs coated by SDS (-39.9 mV) as a representative of negatively charged particle. The fractograms of SeNPs in different membrane materials and MWCOs are presented in Fig. S1 (a) and S1 (b). Due to the higher hydrophobicity of PES membrane as compared with RC membrane that can be explained by their different zeta potential of both membrane materials as mentioned elsewhere (Saenmuangchin and Siripinyanond, 2018, Bendixen et al., 2014), it is clearly shown that the retention times of SeNPs obtained by using two membranes were different (1^{st} peak, see Fig. S1 (a) and S1 (b)). This is correlated with what Bendixen et al. (Bendixen et al., 2014) found for TiO_2 NPs characterization. The shift of retention time can also be due to the different actual channel thickness of both membranes that was calculated by using polystyrene standard particle (Giddings et al., 1992) to be 178 μm for PES and 149 μm for RC membranes. The longer retention time of nanoparticle in the channel will also lead to the likeliness of particle membrane interaction. Considering the particle membrane interaction problem, the positively charge particle would exhibit electrostatic interaction with the negatively charged membrane inside the FlFFF channel, resulting in no elution. In this case, it is interesting that even though SeNPs coated by β-lactoglobulin are positively charged

particle, they were still eluted from the channel. This is due to the slighlty higher channel flow rate as compared to the cross flow rate. The selected cross flow rate is not very high, however, it is strong enough to cause retention without causing irreversible membrane adsorption. This is observed from a release peak (after stopping cross flow) as shown in the fractograms in Fig. S1 (a) and S1 (b).

The release peak (see Fig. S1 (a) and S1 (b) for both of SeNPs with the use of 10 kDa RC and 10 kDa PES membranes was smaller than what was observed with 1 kDa RC and 1 kDa PES membranes. Hence, MWCO is a crucial factor affecting on sample recovery, as the membrane allows the removal of impurities in the sample and also causes particle loss (Kavurt et al., 2015). With 1 kDa RC or 1 kDa PES membrane (lower MWCO), more particles attached on the membrane resulting in higher release peak after stopping cross flow as mentioned in another work by Zulfah and Siripinyanond (Zulfah and Siripinyanond, 2018) for SiO_2 NPs characterization. For size characterization, standard NPs with well-known diameter are needed for checking sensitivity of system (Bendixen et al., 2014, Nischwitz and Goenaga-Infante, 2012). Not only the membrane materials and MWCO are crucial but the type of carrier liquid also needs to be taken into consideration.

2. Effect of carrier liquid to the retention behavior of SeNPs

From the study mentioned above, 10 kDa RC and 10 kDa PES membranes were selected due to the higher elution peak as compared with 1 kDa membranes. The effect of carrier liquid, which were 0.02% FL-70 with 0.02% NaN_3 and 0.02% SDS with 0.02% NaN_3, was observed. FL-70 is normally used as carrier liquid in FlFFF. Bendixen et al. (Bendixen et al., 2014) used SDS as known pure anionic surfactant to modify surface charge of membrane keeping a negative charge on the membrane surface owing to its alkyl chain functional group which is observed from zeta potential value. Three types of SeNPs were investigated including SDS, β-lactoglobulin-, and albumin-stabilized SeNPs.

Fig. S2 (a) and S2 (b) show the effect of using FL-70 with different types of membrane materials. With RC membrane, the retention order for all SeNPs is related with DLS result as presented in Table 4 by which SeNPs coated by SDS eluted sooner than SeNPs coated by proteins. But with the use of PES membrane, SeNPs coated by albumin was not eluted. It is possible to be caused by attractive interaction between PES membrane and albumin. The attractive interaction can be due to electrostatic attraction between the positively charged albumin stabilized SeNPs and negatively charged membrane, and also the hydrophobic interaction between PES membrane and albumin as protein. On the contrary, these attractive interactions were not as strong as in the case of β-lactoglobulin stabilized SeNPs (23.3 mV) as it was less positive as compared to albumin (35.8 mV). In addition, albumin was more hydrophobic owing to its larger molecular weight (18.4 kDa for β-lactoglobulin and 66.5 kDa for albumin). This observation was in agreement with what was previously reported by Salgin et al. (Salgın et al., 2006) that the bovine serum albumin (BSA) showed largest adsorption onto the PES membrane, and Kelly et al. (Kelly and Zydney, 1994) that BSA was easy to aggregate during filtration with the increasing pH. In this study, the pH of FL-70 carrier liquid is approximately 8-9. In contrast with SeNPs coated by β-lactoglobulin which is also protein as albumin, Kim et al. (Kim and Shin, 2015) reported hydrophobic interaction of β-lactoglobulin and PES membrane above pH 7.5. In our finding, due to the difference in MW of both proteins, SeNPs coated by albumin with higher MW than β-lactoglobulin retained in the vicinity of PES membrane because of the applied flow field force. Increasing the channel flow rate or decreasing the cross flow rate can help lessen the problem of particle membrane adsorption and is suggested for further observation.

By using SDS as carrier liquid, the different retention behavior was observed as shown in Fig. S2 (c) and S2 (d). The retention order was not correlated well with DLS analysis, as albumin stabilized SeNPs eluted earlier than SDS stabilized SeNPs when using

10 kDa RC membrane, though their elution peaks were quite good. This phenomena could not be explained based on the hydrophobic interaction only, but the composition of carrier liquid also plays important role. From all these results, 0.02% FL-70 with 0.02% NaN_3 and 10 kDa RC membrane were selected as suitable carrier liquid and membrane, respectively, for size characterization to provide reliable retention times and to achieve an accurate size information.

3. Relative fractionation recovery

Fractionation recovery (see equation below) is another parameter to check the performance of FlFFF system and to evaluate the interaction of membrane materials and carrier liquids.

$$R\ (\%) = \frac{S}{S_0} \times 100\%$$

Where S = peak area obtained with cross flow and S_0 = peak area obtained without cross-flow.

A comparison of relative fractionation recovery in different membrane materials and carrier liquids for SeNPs is displayed in Fig.S3 (a) and S3 (b). The fractionation recovery decreased as the size increased ($SeNPs_{albumin} < SeNPs_{\beta\text{-lactoglobulin}} < SeNPs_{SDS}$). This is due to the fact that the largest particle will be closest to the accumulation wall, leading to interact more with the membrane and thereby reducing the fractionation recovery. SeNPs coated by proteins can be eluted because of the addition of sodium azide in the carrier liquid reducing the protein-membrane adsorption (Kim and Shin, 2015). However, SeNPs coated by albumin showed the poor fractionation recovery with the use FL-70 as carrier liquid and PES as membrane material (See Fig. S2 (a)) despite the addition of sodium azide with the reasons described earlier.

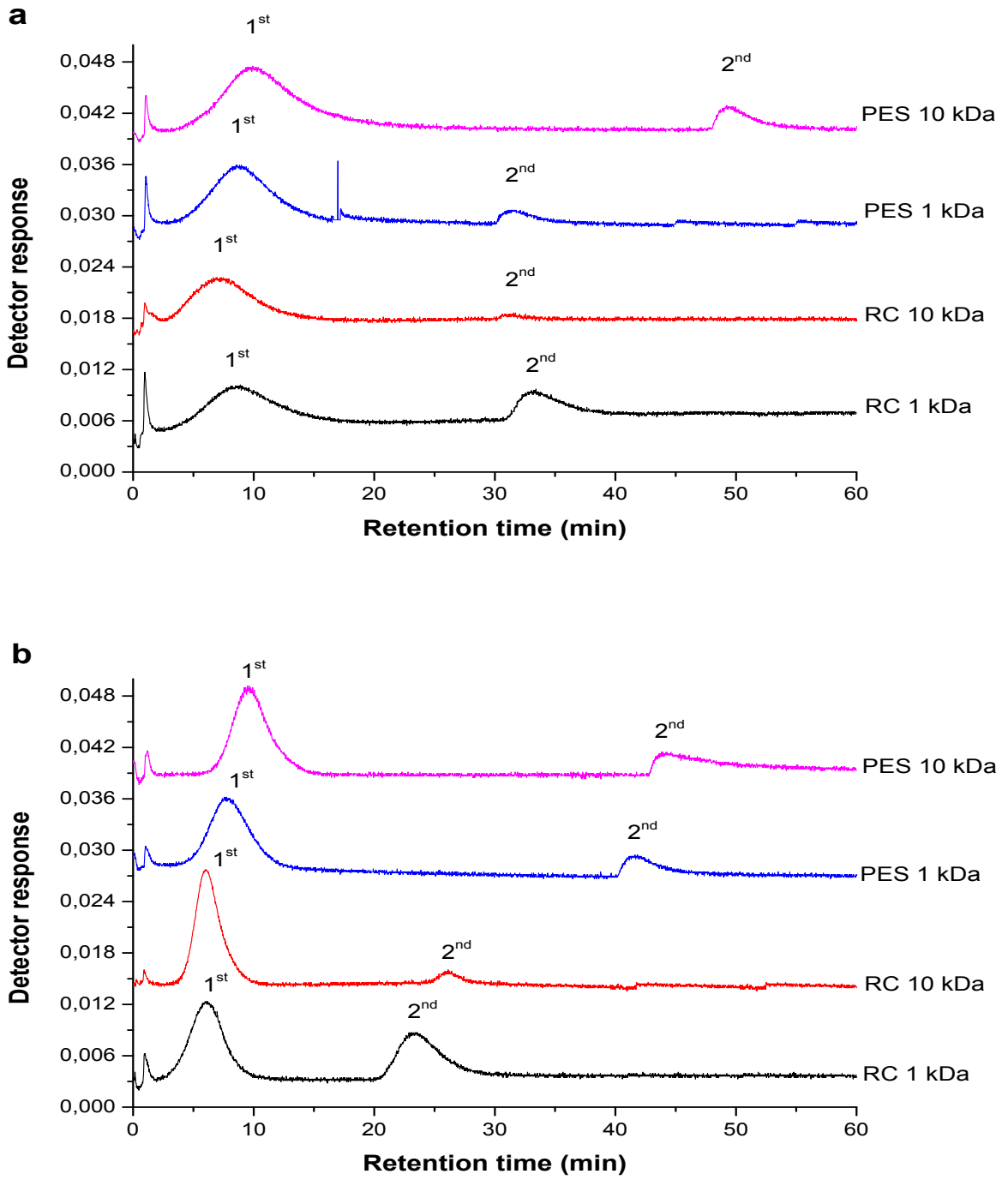

Figure S1. Influence of different membrane materials and membrane molecular weight cut offs: RC 1 kDa (black line); RC 10 kDa (red line); PES 1 kDa (blue line); and PES 10 kDa (pink line) by using 0.02% FL-70 + 0.02% NaN_3on the peak elution of SeNPs synthesized with various types of stabilizing agents: (a) β-lactoglobulin (sample H); and (b) sodium

dodecyl sulfate (SDS) (sample A). (1st) with cross flow applied ; (2nd) without cross flow applied

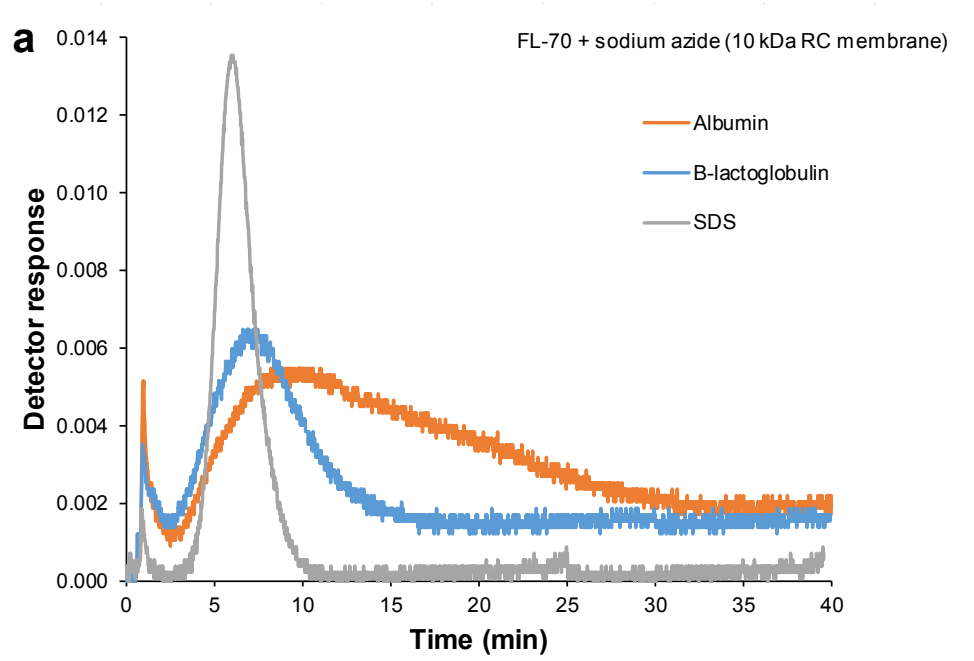

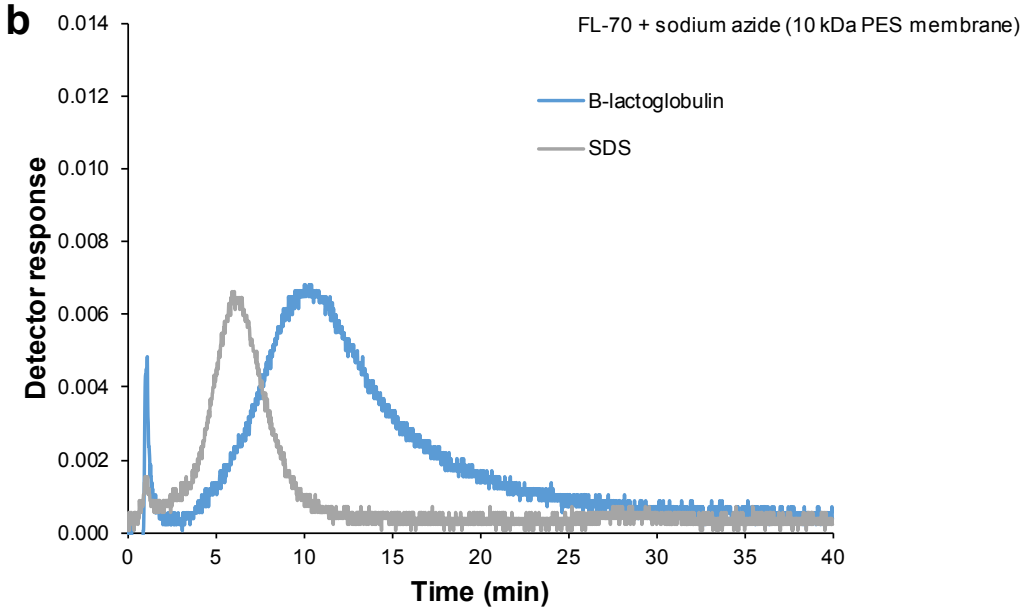

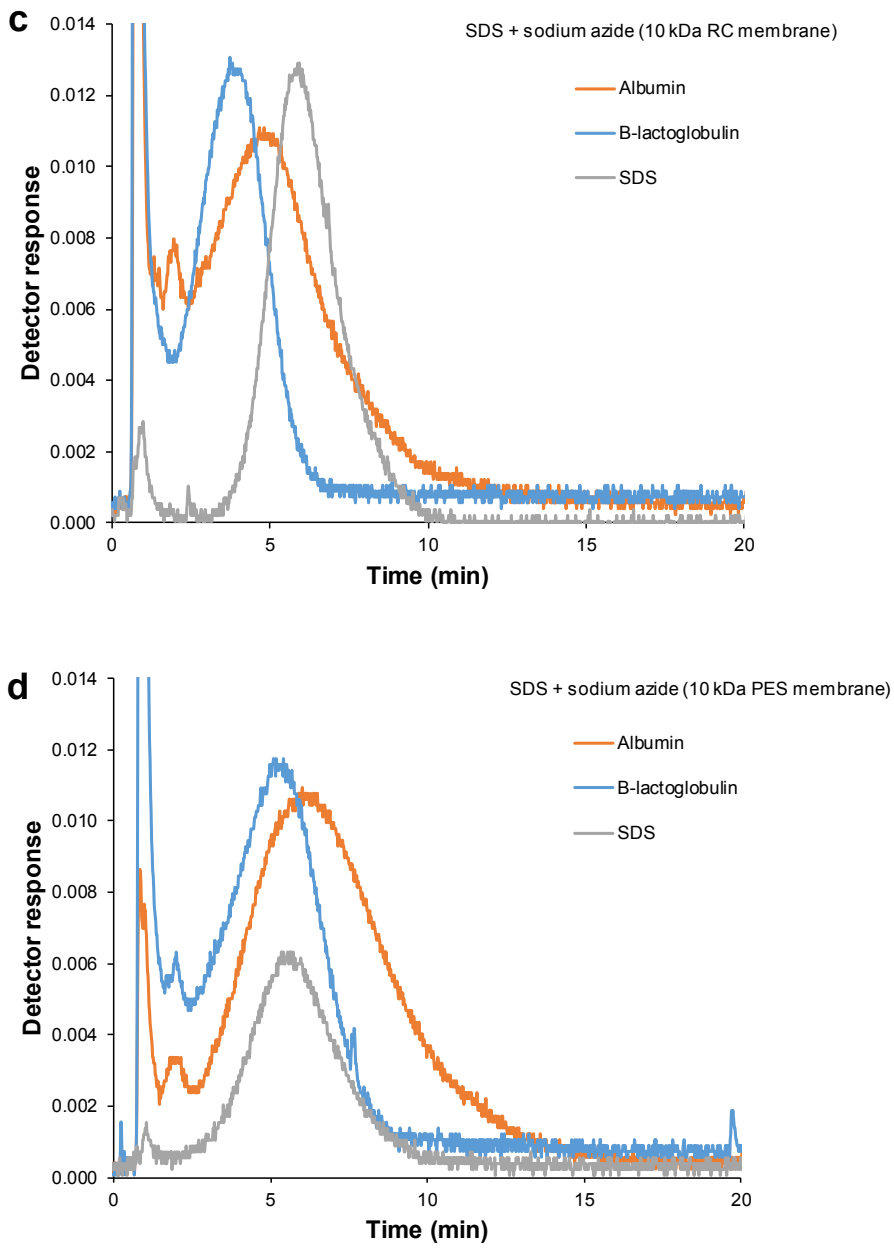

Figure S2. Influence of different carrier liquids: (a) and (b) 0.02% FL-70 with 0.02% sodium azide RC 10 kDa and PES membrane; (c) and (d) 0.02% SDS with 0.02% sodium azide RC 10 kDa and PES membrane on the retention behavior of SeNPs synthesized with various types of stabilizing agents, i.e., β-lactoglobulin (sample H; blue line); SDS (sample A; gray line); and albumin (sample I; orange line).

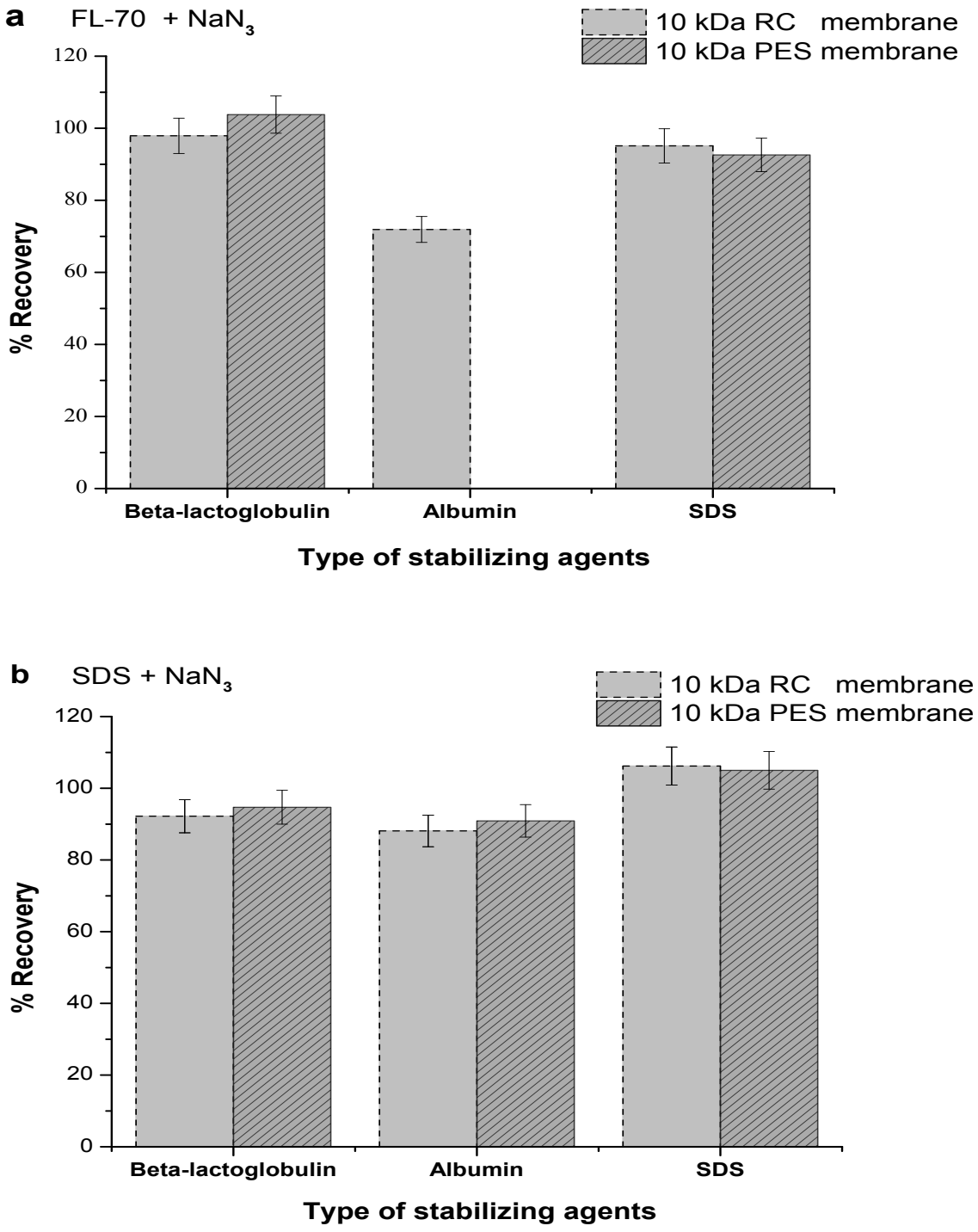

Figure S3. Relative fractionation recovery of SeNPs synthesized (sample A, sample H, sample I) obtained from two different carrier liquids: (a) 0.02% FL-70 with 0.02% sodium azide; and (b) 0.02% SDS with 0.02% sodium azide with the use of 10 kDa RC and 10 kDa PES membrane.

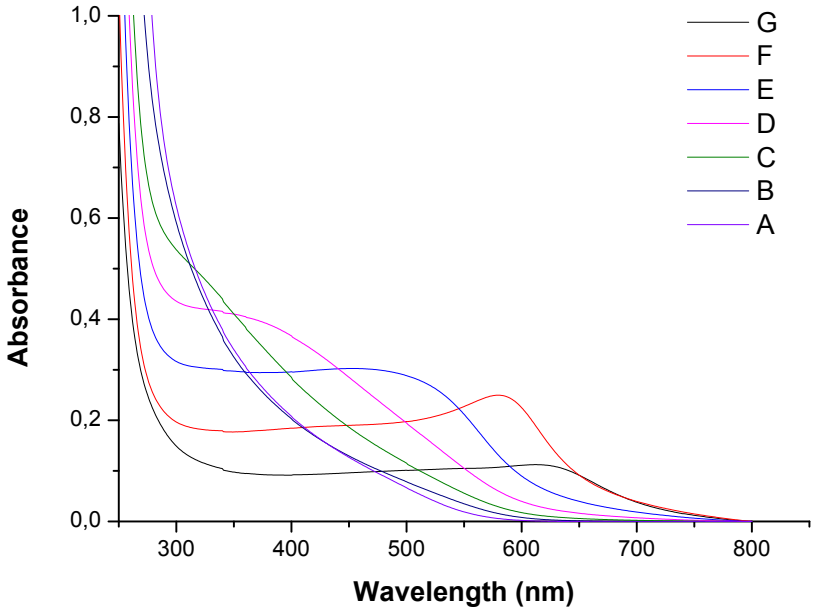

Figure S4. Absorption spectra of the synthesized SeNPs with different amounts of thiosulfate as reducing agent ; (A) 3.0 mL (B) 0.8 mL (C) 0.5 mL (D) 0.4 mL (E) 0.3 mL (F) 0.2 mL and (G) 0.1 mL.

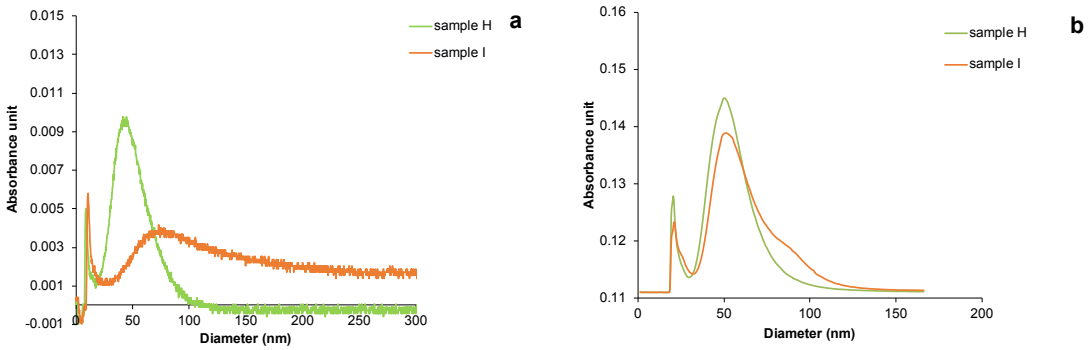

Figure S5. Diameter of SeNPs coated by proteins observed by (a) Sy-FlFFF and (b) Asy-FlFFF after converting the retention time (Fig.3) into the hydrodynamic diameter.

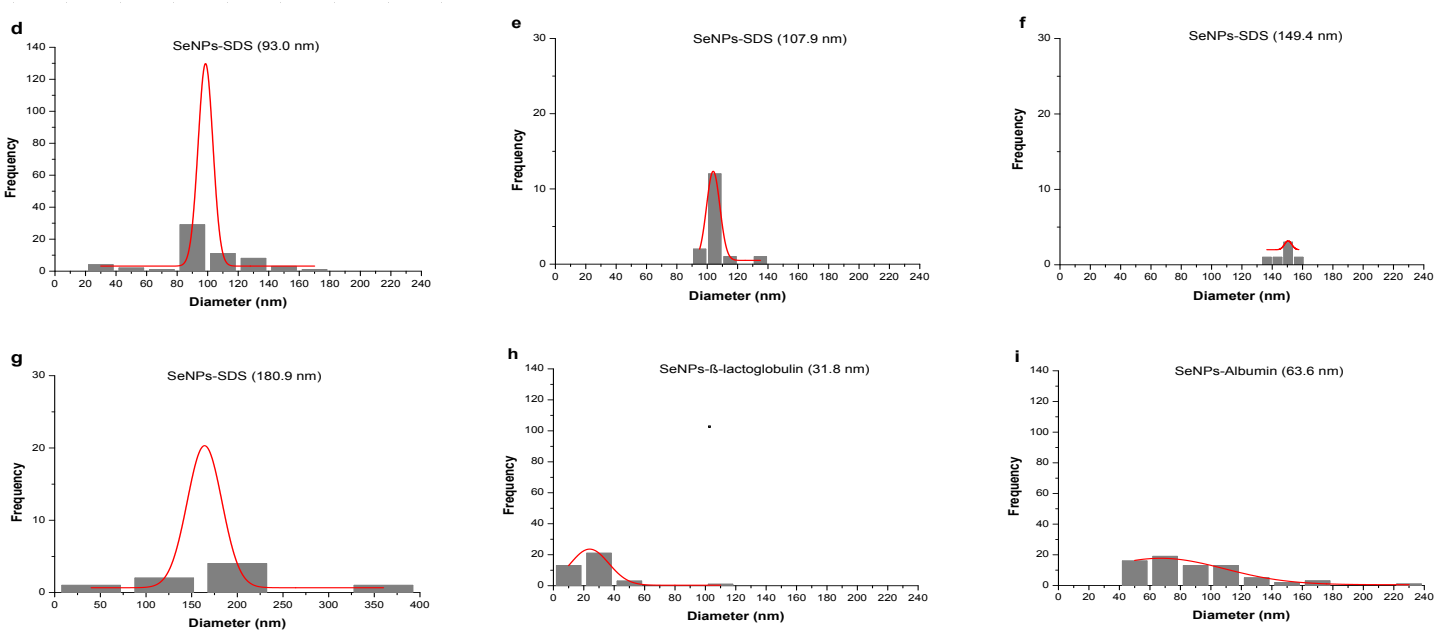

Figure S6. Size distributions of SeNPs-SDS (D-G) and SeNPs-protein (H-I) from TEM technique

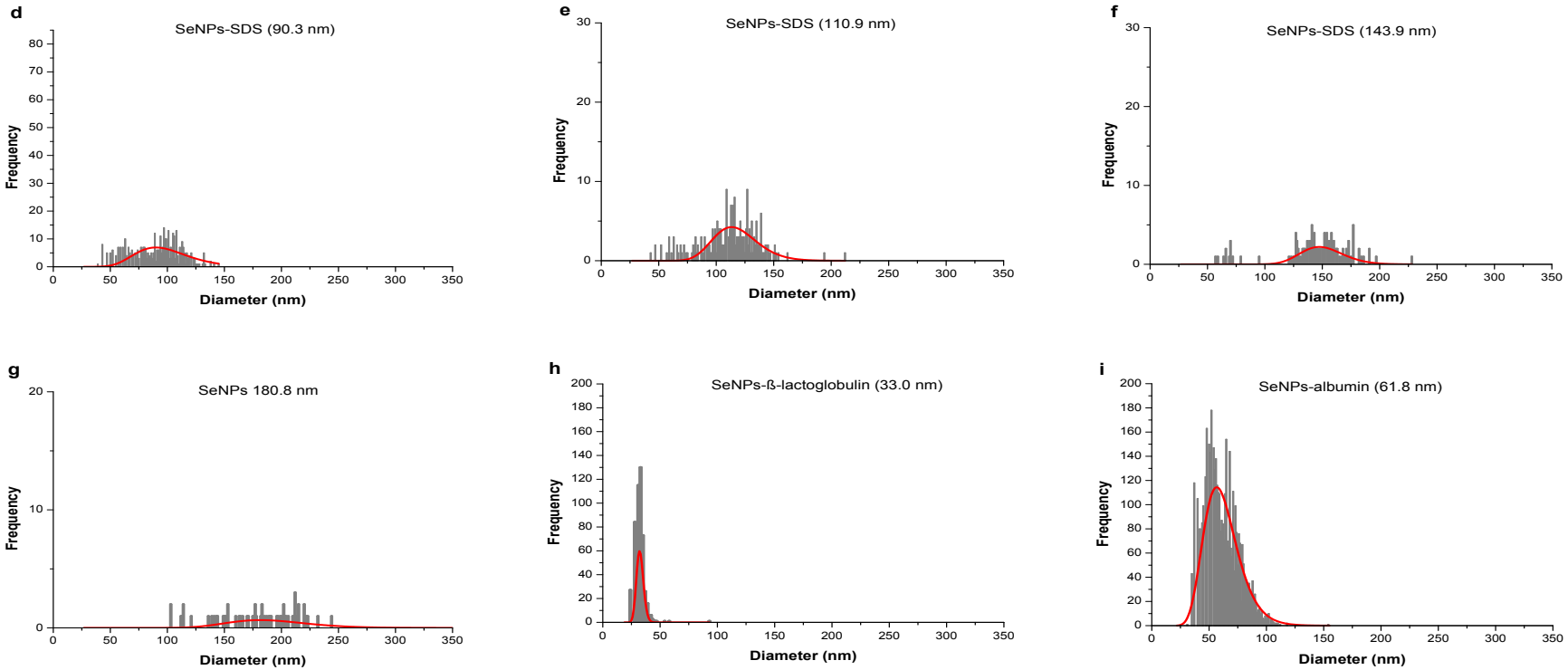

Figure S7. Size distributions of SeNPs-SDS (D-G) and SeNPs-protein (H-I) from SP-ICP-MS

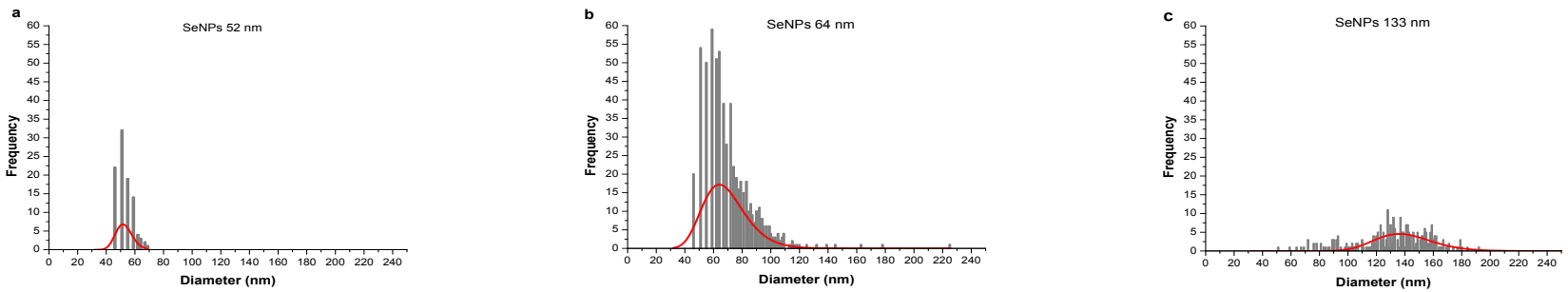

Figure S8. Size distributions of SeNPs-SDS from SP-ICP-MS

References

Bendixen N, Losert S, Adlhart C, Lattuada M, Ulrich A. Membrane–particle interactions in an asymmetric flow field flow fractionation channel studied with titanium dioxide nanoparticles. J Chromatogr A. 2014;1334:92-100.

Giddings JC, Williams PS, Benincasa, MAJ. Rapid breakthrough measurement of void volume for field-flow fractionation channels. J Chromatogr. 1992;627:23-35.

Kavurt UB, Marioli M, Kok WT, Stamatialis D. Membranes for separation of biomacromolecules and bioparticles via flow field-flow fractionation. J Chem Tech Biotech. 2015;90**:**11-18.

Kelly ST, Zydney AL. Effects of intermolecular thiol–disulfide interchange reactions on bsa fouling during microfiltration. Biotech Bioeng. 1994;44**:**972-982.

Kim JT, Shin GH. Adsorption behavior of β-lactoglobulin onto polyethersulfone membrane surface. J Adhesion Sci Tech. 2015;29**:**2245-2255.

Nischwitz V, Goenaga-Infante H. Improved sample preparation and quality control for the characterisation of titanium dioxide nanoparticles in sunscreens using flow field flow fractionation on-line with inductively coupled plasma mass spectrometry. J Anal At Spectrom. 2012;27**:**1084-1092.

Saenmuangchin R, Siripinyanond A. Flow field-flow fractionation for hydrodynamic diameter estimation of gold nanoparticles with various types of surface coatings. Anal Bioanal Chem. 2018;410:6845-6859.

Salgın S, Takaç S, Özdamar TH. Adsorption of bovine serum albumin on polyether sulfone ultrafiltration membranes: determination of interfacial interaction energy and effective diffusion coefficient. J Membrane Sci. 2006;278**:**251-260.

Zulfah NL, Siripinyanond A. Investigation of tin adsorption on silica nanoparticles by using flow field-flow fractionation with offline inductively coupled plasma mass spectrometry. J Anal Sci Tech. 2018;9**:**19.